10 Particle Physics with LHCb

J. Anderson, R. Bernet, A. Bursche, A. Büchler (until November 2011), N. Chiapolini, M. De Cian, Ch. Elsasser, K. Müller, Ch. Salzmann, S. Saornil, N. Serra, St. Steiner, O. Steinkamp, U. Straumann, M. Tobin, M. Tresch, A. Vollhardt

The full LHCb collaboration consists of 54 institutes from Brazil, China, France, Germany, Ireland, Italy, the Netherlands, Poland, Romania, Russia, Spain, Switzerland, Ukraine, the United Kingdom and the United States of America.

(LHCb - Collaboration)

LHCb is the smallest of the four experiments at the Large Hadron Collider (LHC). Its main goal is the indirect search for New Physics (NP) through precision measurements of CP violating phases and rare heavy-quark decays. The measurements are complementary to direct searches also performed at LHC by CMS and ATLAS. Of particular interest are processes that are strongly suppressed in the Standard Model (SM), such as flavour-changing neutral current $b \to s$ transitions. Since CP violating asymmetries are generated by diagrams that involve internal loops with virtual particles, they can be very sensitive to NP contributions.

10.1 The LHCb detector

The LHCb detector[1] is a single-arm forward spectrometer exploiting best the forward peaked $b\bar{b}$ production cross section at the LHC. The detector covers polar angles between 15 and 300 mrad in the bending plane of the spectrometer magnet and up to 250 mrad in the non-bending plane. This acceptance corresponds to a pseudorapidity coverage in the range 1.9 to 4.5. The detector has an excellent vertex and momentum resolution needed to separate primary and secondary vertices, provides good invariant mass resolution, and is able to trigger on particles with transverse momentum, p_T, down to a few GeV only. Two RICH detectors allow discrimination between pions and kaons over a wide momentum range. The detector and its performance have been described in previous annual reports [2].

10.1.1 Detector performance and operation

LHCb was designed to operate at a centre-of-mass energy $\sqrt{s} = 14$ TeV, 2622 colliding bunches and an average instantaneous luminosity of $2 \times 10^{32}\text{cm}^{-2}\text{s}^{-1}$. Under these conditions the events are dominated by a single pp interaction per bunch crossing giving an average number of visible interactions, μ, equal to 0.4. However, the data collected in 2011 was taken at $\sqrt{s} = 7$ TeV and luminosities up to $4 \times 10^{32}\text{cm}^{-2}\text{s}^{-1}$ leading to $\mu \simeq 1.6$. These conditions were achieved using a process called *luminosity levelling*: the luminosity delivered to LHCb was kept constant throughout the length of a fill by gradually reducing the beam separation in the vertical plane around the LHCb interaction point. This automatic procedure allowed LHCb to record most of the data at a luminosity around $4 \times 10^{32}\text{cm}^{-2}\text{s}^{-1}$ which is twice the design value. A total of around 11 billion events were collected in 2011 for physics analysis.

The experiment recorded around 1.1 fb^{-1} of pp collisions during the 2011 run with a global operation efficiency over 90%. The polarity of the LHCb spectrometer magnet was reversed several times to minimise possible systematic effects due to detector asymmetries. The LHC will run at a higher centre-of-mass energy, $\sqrt{s} = 8$ TeV, during 2012 and the target integrated luminosity for LHCb is 1.5 fb^{-1}.

An excellent vertex resolution is required for the high level trigger and for many physics analyses. The LHCb vertex detector has an internal alignment better than 5 μm and a single hit position resolution of 4 μm has been achieved for

the innermost readout strips. High momentum and invariant mass resolutions are essential for the suppression of combinatorial backgrounds. Measured spatial resolutions in the tracking system are close to the values expected from simulation. The invariant mass resolution obtained for $J/\Psi \to \mu^+\mu^-$ decays is 12.7 MeV/c^2 close to the simulated 12.1 MeV/c^2. The particle identification performance has been studied using tag-and-probe methods on $\phi \to K^+K^-$, $K^0_s \to \pi^+\pi^-$ and $\Lambda \to p\pi$ decays and agrees with the results from the simulation over the full momentum range.

10.1.2 Tracker Turicensis: operation and performance

N. Chiapolini, C. Salzmann, S. Saornil, M. Tobin

The Tracker Turicensis (TT) was designed and built at the Physics Institute and has been described in previous annual reports [2]. Modules that originally had a problem with broken bond wires were successfully repaired during the winter shutdown 2010. During 2011 99.8% of the 143360 detector channels were operating which is the highest reliability figure of any silicon tracking detector at the LHC. The continued stable and efficient operation of the TT and the monitoring of its performance including ageing effects are the responsibility of S. Saornil and M. Tobin. The software alignment of the detector is performed by N. Chiapolini and C. Salzmann.

10.2 Physics Results

10.2.1 CP violation in B decays

Mixing in the $B_s - \overline{B}_s$ system is described by the mass difference Δm_s, the decay width difference $\Delta\Gamma_s$, and a single CP violating phase ϕ_s. All three observables can substantially deviate from SM predictions if NP contributes. The LHCb experiment recently extracted the present most accurate values for Δm_s [3] by studying $B_s \to D_s(3)\pi$ and for the other two parameters from $B_s \to J/\psi\phi$ [4]:

$$\begin{aligned} \Delta\Gamma_s &= 0.116 \pm 0.018 \pm 0.006 \text{ ps}^{-1} \\ \phi_s &= -0.001 \pm 0.101 \pm 0.027 \text{ rad} \end{aligned}$$

in agreement with SM predictions ($\Delta\Gamma_s^{SM} = 0.087 \pm 0.021$ ps^{-1} [5] and $\phi_s^{SM} = 0.036 \pm 0.02$ rad [6])[10]. The 5σ deviation of $\Delta\Gamma_s$ from 0 represents the first significant observation of its non-zero value. In addition, a long-standing sign ambiguity in $\Delta\Gamma_s$ has been resolved by separating the S-wave and P-wave contributions to the decay $B_s \to J/\psi K^+K^-$ [7].

In the B_d system the mixing phase is sizeable and can be associated with the angle β of the Unitarity Triangle, while the width difference is small. At present there is a striking discrepancy between the measured values of $\sin 2\beta$ using $B_d \to J/\psi K^0_S$ and the branching ratio $\mathcal{B}(B \to \tau\nu)$ [8, 9]. In the SM these observables can be related through the CKM matrix element V_{ub}. To understand this tension, it will be important to control the contribution of doubly Cabibbo-suppressed penguin diagrams in the $B_d \to J/\psi K^0_S$ decay. Its U-spin partner, the decay $B_s \to J/\psi K^0_S$, can be used to measure these effects. LHCb recently found $\mathcal{B}(B_s \to J/\psi K^0_S) = (3.29 \pm 0.51 \pm 0.33) \times 10^{-5}$ [10].

The photon polarisation in $b \to s\gamma$ transitions can be determined by CP asymmetry measurements. This observable probes extensions of the SM involving right-handed currents. Important milestones in this measurement are the determination of the ratio of the branching ratios [11]

$$\frac{\mathcal{B}(B_d \to K^*\gamma)}{\mathcal{B}(B_s \to \phi^*\gamma)} = 1.12 \pm 0.08^{+0.11}_{-0.09}$$

and the world's most precise measurement of direct CP asymmetry in the decay $B_d \to K^*\gamma$ [12].

A precise determination of the angle γ of the Unitarity Triangle from tree level decays is another crucial ingredient to test the CKM paradigm. The angle γ is the weak phase between the elements of the CKM matrix V_{cb} and V_{ub} and has been studied by LHCb in the decay $B^+ \to D^0K^+$, where the D^0 meson subsequently decays

[10] For all the results the first uncertainty is statistical and the second systematic.

in CP-eigenstates or where the D^0 meson decays in the Cabibbo-favoured $K^-\pi^+$ and in the doubly Cabibbo-suppressed $K^+\pi^-$ states. LHCb has observed the doubly Cabibbo-suppressed decay $B^+ \to (K^-\pi^+)_D K^+$ with 10σ significance and has established the CP violation in $B^+ \to D^0 K^+$ at 5.8σ [13].

The angle γ can also be determined from the loop mediated decays $B_{d,s} \to h^+h^-$, where h stands for a kaon or a pion. A significant difference in the value of γ from tree level and loop dominated decays would be a clear sign of NP. An important milestone in the determination of γ from loop processes is the first measurement of the time-dependent CP asymmetry in the decay $B_s \to K^+K^-$, leading to the determination of the direct and mixing asymmetries [14]:

$$\begin{aligned} A_{KK}^{\rm dir} &= 0.02 \pm 0.18 \pm 0.04\,, \\ A_{KK}^{\rm mix} &= 0.17 \pm 0.18 \pm 0.05\,. \end{aligned}$$

10.2.2 CP violation in Charm

Mixing in the D^0 meson is induced by down-type quarks contributing to the box diagrams, which leads to a strong cancellation; therefore this mixing process is strongly suppressed. Mixing induced and direct CP asymmetries in charm decays are expected to be small, but can be highly enhanced by NP contributions. CP violation in D^0 mixing can be measured by comparing the effective lifetimes of D^0 and $\overline{D}^0$ decaying in CP eigenstates. The asymmetry of the lifetimes defines A_Γ. This analysis has been performed with a fraction of the data, leading to the result [15]

$$A_\Gamma = (-5.9 \pm 5.9 \pm 2.1) \times 10^{-3}.$$

For the moment no sign of CP violation in this measurement has been observed. The difference in the CP asymmetry of $D^0 \to \pi^+\pi^-$ and $D^0 \to K^+K^-$ has also been measured [16] :

$$\Delta A_{CP} = (-8.1 \pm 2.1 \pm 1.1) \times 10^{-3}\,,$$

which is the first evidence of CP violation in the charm sector. The traditional view that CP violation in these channels does not exceed 10^{-3} in the SM has been questioned recently [17–19] and it is not yet clear if this level of CP violation can be accommodated in the SM.

10.2.3 Rare decays

Searches for the total lepton number violating decay $B^+ \to h^-\mu^+\mu^+$, where h is a pion, a kaon or a D meson, resulted in todays world's best upper limits [20, 21].

The decays $B_{s,d} \to \mu^+\mu^-\mu^+\mu^-$ have branching ratios below 10^{-10} in the SM but could be enhanced in models involving exotic scalar particles. Searches for these decays have been performed at LHCb for the first time, leading to [22]:

$$\begin{aligned} \mathcal{B}(B_s \to \mu^+\mu^-\mu^+\mu^-) &< 1.3 \times 10^{-8} \\ \mathcal{B}(B_d \to \mu^+\mu^-\mu^+\mu^-) &< 5.4 \times 10^{-9} \end{aligned}$$

at 95% CL. The world's best limit $\mathcal{B}(D^0 \to \mu^+\mu^-) < 1.3 \times 10^{-8}$ (95% CL) has also been set [23].

The $b \to dll$ transitions are suppressed by a factor $|V_{td}/V_{ts}|$ with respect to $b \to sll$. Transitions $b \to dll$ have been observed for the first time at $\mathcal{B}(B^+ \to \pi^+\mu^+\mu^-) = (2.4 \pm 0.6 \pm 0.2) \times 10^{-8}$ in agreement with the SM prediction. This is to date the rarest B-decay ever observed.

10.2.4 The very rare decays $B_s^0 \to \mu^+\mu^-$ and $B^0 \to \mu^+\mu^-$

A. Büchler, Ch. Elsasser, N. Serra and O. Steinkamp

Our group is deeply involved in this key LHCb measurement. In the decays $B_s^0 \to \mu^+\mu^-$ and $B^0 \to \mu^+\mu^-$ NP contributions might be of the same order of magnitude as the contributions from the SM. Hence, lowering the experimental uncertainties in these branching fractions largely reduces the allowed parameter space in various NP models.

The first LHCb results, based on the 2010 data set [24], came already close to the known upper limits set by CDF [25]. In the case of $B_s^0 \to \mu^+\mu^-$ the limit was still an order of magnitude above the SM prediction $(3.2 \pm 0.2) \times 10^{-9}$ [26].

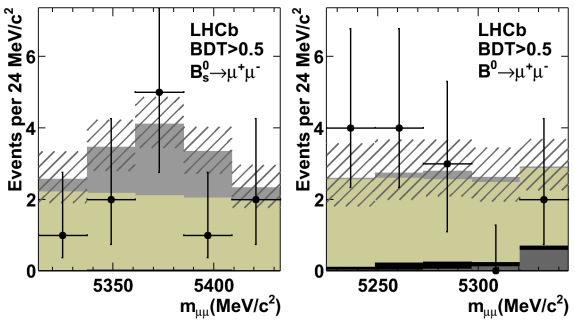

FIG. 10.1 – *Distribution of selected candidates (black points) in the (left) $B_s^0 \to \mu^+\mu^-$ and (right) $B^0 \to \mu^+\mu^-$ mass window, and expectations for, from the top, $B^0 \to \mu^+\mu^-$ SM signal (gray), combinatorial background (light gray), $B^0 \to h^+h'^-$ background (black), and cross-feed of the two modes (dark gray). The hatched area depicts the uncertainty on the sum of the expected contributions.*

The analysis was repeated on the full 2011 data set which corresponds to 1 fb^{-1}. Figure 10.1 shows as a result the mass distribution of the selected $B_s^0 \to \mu^+\mu^-$ and $B^0 \to \mu^+\mu^-$ candidates which gave the following limits at 95% C.L.[27] :

$$\begin{aligned} \mathcal{B}(B_s^0 \to \mu^+\mu^-) &< 4.5 \times 10^{-9} \\ \mathcal{B}(B^0 \to \mu^+\mu^-) &< 1.0 \times 10^{-9} \ . \end{aligned}$$

As the results are still in agreement with the SM predictions, they heavily constrain NP models [28].

The main activity of our group in this analysis is the calibration of the di-muon invariant mass which is the main variable distinguishing signal from background. The invariant mass resolution for B_s^0 and B^0 was determined by Ch. Elsasser by interpolating between the values for the resonances J/ψ, $\psi(2S)$, $\Upsilon(1S)$, $\Upsilon(2S)$ and $\Upsilon(3S)$ and by considering the resolution of the exclusive $B_{(s)}^0 \to h^+h^-$ decays where $h^\pm$ is a kaon or a pion. These two results are in perfect agreement. An alternative method, which determines an event-by-event invariant mass error was developed by A. Büchler. It propagates the errors on the muon momenta and the opening angle between the two muons obtained from the track and vertex fit to a mass error.

Ch. Elsasser is also determining the effective masses of B_s^0 and B^0 as well as the impact of final state radiation on the invariant mass distribution. Finally, exclusive $B_{(s)}^0 \to h^+h^-$ decays are also used to estimate systematic uncertainties in a classifier based on kinematical and topological variables, which is used as an alternative discriminator between signal and background.

10.2.5 Other very rare B-decays

Ch. Elsasser, N. Serra and O. Steinkamp

Thanks to the high momentum resolution and the efficient particle identification as well as the large number of B-mesons LHCb reaches an unprecedented sensitivity to other very rare B-decays such as $B_{(s)}^0 \to \tau^+\tau^-$ and to Lepton Flavour Violating decays such as $B_{(s)}^0 \to e^\pm\mu^\mp$ and $B_{(s)}^0 \to \mu^\pm\tau^\mp$ which are practically forbidden in the SM but can be accommodated in several NP scenarios. In the Pati-Salam model [29], for example, leptoquark exchange mediates these decays already at tree level. The decay $B_{(s)}^0 \to \tau^+\tau^-$ is less helicity suppressed than $B_{(s)}^0 \to \mu^+\mu^-$ because of the higher lepton mass.

Our group will study these decay channels, profiting from the experience gained in the $B_{(s)}^0 \to \mu^+\mu^-$ analysis. In a first stage the focus lies on the study of the τ-reconstruction and -selection using Monte Carlo simulations and more frequent decays into τ's such as $Z \to \tau^+\tau^-$.

10.2.6 $B^0 \to K^\star\mu^+\mu^-$

M. De Cian, N. Serra and M. Tresch

The rare decay $B^0 \to K^\star\mu^+\mu^-$ proceeds via flavour-changing neutral currents which makes it of particular interest as its angular distributions and differential branching fraction are sensitive to many potential NP contributions. The forward-backward asymmetry A_{FB}, described by the opening angle between the μ^- and the B^0 in the $\mu^+\mu^-$ rest frame, has attracted special attention. In the SM A_{FB} changes sign at a well defined value of q^2, the di-muon invariant mass squared. This zero-crossing point is essentially free of hadronic uncer-

tainties and can therefore be very well predicted theoretically. With the full 2011 dataset, LHCb performed an angular analysis and a measurement of the differential branching fraction, which yield the worlds most precise results of all observables involved [30] in good agreement with the SM values. The experimental precision is still statistically limited and not yet sensitive to NP contributions.

Our group is responsible for the determination of the zero-crossing point of A_{FB}, which was measured for the first time [30] (see Fig. 10.2). The result was extracted using a novel "unbinned counting" technique which avoids biases introduced by the range in which the zero-crossing point is looked for or by strong assumptions on the shape of A_{FB}. This shape is in good agreement with the result from a simple counting analysis of the same data. The uncertainty on the zero-crossing point was estimated using a data-driven approach. The result is fully compatible with predictions from the SM.

To account for possible biases introduced by detector acceptance and reconstruction effects, a correction procedure was developed. Correction factors are determined using simulated events, which have been corrected for known discrepancies between measurement and simulation. Ch. Salzmann played an important role in evaluating the agreement between measurement and simulation in the kinematically similar decay $B^0 \to J/\Psi(\mu^+\mu^-)K^\star$. This decay shares the final state with $B^0 \to K^\star\mu^+\mu^-$ but is more abundant by a factor of 50. He studied several techniques to correct the simulated distributions and, together with M. De Cian, also determined efficiencies for particle identification. The measurement of tracking efficiencies using a tag-and-probe approach, which was developed independently, was needed as a further input for the efficiency studies [32].

Due to limited statistics of the 2011 dataset, not all possible observables could be accessed in the angular analysis. The remaining ones can be measured using a technique similar to the one developed for A_{FB}. Our group is investigating how to extract these quantities which are well predicted in the SM.

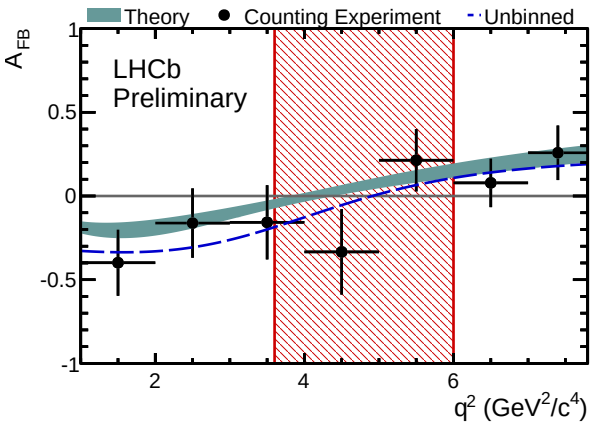

FIG. 10.2 – *A_{FB} as a function of q^2. The dashed blue line corresponds to the "unbinned counting" experiment, the turquoise band is the theoretical prediction [31]. The data points represent the result of counting forward and backward events showing the statistical uncertainty only. The red hatched region shows the observed 68% confidence interval for the zero-crossing point.*

10.2.7 W, Z and low mass Drell-Yan production

J. Anderson, A. Bursche, N. Chiapolini, and K. Müller

Measurements of W, Z and low mass Drell-Yan production in the forward region constitute a test of QCD at LHC energies and will provide valuable input to the knowledge of the parton density functions (PDF) of the proton in a kinematic region uniquely accessible by LHCb. Measurements at LHCb are sensitive to Bjorken-x values as low as 8×10^{-6} where x is the momentum fraction carried by the struck quark. Perturbative QCD predictions are available at next-to-next-to-leading order (NNLO).

- W and Z production

W and Z production cross sections and their ratios have been measured by LHCb using the $W \to \mu\nu$ and $Z \to \mu\mu$ decay channels. Results have already been presented at conferences and are being published [33].

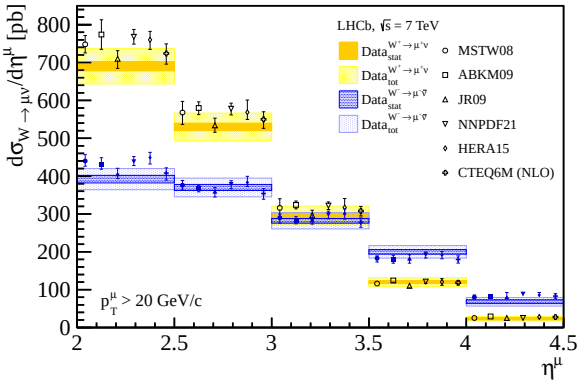

FIG. 10.3 – *Pseudorapidity dependence of the $W \to \mu\nu_\mu$ production cross-section. The dark shaded bands correspond to the statistical uncertainties, the light hatched band to the statistical and systematic uncertainties added in quadrature. The superimposed NNLO (NLO) predictions are displaced horizontally for better presentation.*

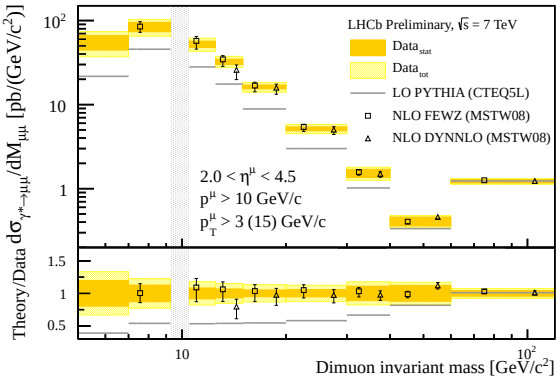

FIG. 10.4 – *Differential cross-section for $\gamma^\star \to \mu\mu$ as a function of $M_{\mu\mu}$. The dark shaded (orange) bands correspond to the statistical uncertainties, the light shaded (yellow) band to the statistical and systematic uncertainties added in quadrature. Superimposed are the PYTHIA predictions and two NLO predictions.*

Our group was largely involved in these measurements by determining the detection efficiencies, estimating background contaminations, and determining theoretical predictions. While the analysis of the Z decaying into two muons is almost background free, there is significant background to the $W \to \mu\nu_\mu$ analysis since only one muon is observed. Backgrounds from semileptonic heavy flavour decays or pions or kaons misidentified through decay-in-flight or punch-through (QCD backgrounds) are reduced by requiring the muon to be isolated. Further background arises from electroweak processes. The $W \to \mu\nu_\mu$ signal yield has been determined from fits to the p_{T}^{μ} spectra of positive and negative muons.

Figure 10.3 shows the differential W^+ and W^- cross section as a function of the muon pseudorapidity. The inclusive cross-section for W^+ is larger than for W^-, explained by the excess of u over d quarks in the proton. The W cross-sections strongly vary as a function of the pseudorapidity of the charged lepton, and at high pseudorapidities the W^- is larger than the W^+ cross-section as expected from the different helicity dependences. The results are in agreement with theoretical predictions calculated at NNLO with the program DYNNLO [34] with six recent parametrisations for the PDFs. Most systematic uncertainties cancel in the ratio $R_W \equiv \sigma(W^+)/\sigma(W^-)$ which is measured with a precision of 1.7% which is below the theoretical uncertainty.

The analysis of electroweak boson production is being extended to events containing jets in the final state (A. Bursche). These events are sensitive to the gluon content in the proton. The dominant uncertainty originates in the jet energy scale. The study of jets is new for LHCb and A. Bursche contributed significantly to their definition and calibration.

- Low mass Drell-Yan production

Drell-Yan cross-sections are measured in the dimuon channel [35]; the analysis is performed by the Zurich group (J. Anderson, N. Chiapolini, K. Müller). While the high $M_{\mu\mu}$ region is very clean, towards low masses QCD backgrounds set in. At low masses there is an additional contribution from the radiative tail of the Υ. The signal yield is extracted from a fit to the muon isolation distribution which is defined as the fraction of the transverse momentum of the jet which contains the muon, carried by the muon. Whereas templates for the heavy flavour and misidentification backgrounds are extracted from data, the signal and the Υ background shapes are taken from simulation. The signal yield

varies between 7% in the lowest and more than 99% in the highest mass bin.

Figure 10.4 compares the measured differential cross-section as a function of the di-muon invariant mass with Monte Carlo predictions from PYTHIA and NLO calculations. The NLO predictions agree well with the measurement but PYTHIA predictions are too low. Using the full 2011 dataset will lead to a large reduction of the systematic uncertainties at low masses.

10.3 Summary and Outlook

The LHCb experiment has performed very well throughout the 2011 LHC run. About 1 fb^{-1} of data have been recorded, with a data taking efficiency exceeding 90%. Key performance parameters match or are close to expectations from simulation studies. The LHCb detector produces high quality results which is reflected in more than 30 publications and many more conference contributions to various physics topics in the past year. LHCb has already shown some world best and world first measurements of B-hadron branching ratios and considerably reduced the parameter space for many models beyond the SM.

[1] A. A. Alves Jr. *et al.* [LHCb collaboration], JINST 3 S08005 (2008).

[2] Physik-Institut, University of Zürich, Annual Reports 1996/7 ff.; available at *http://www.physik.uzh.ch/reports.shtml*.

[3] R. Aaij *et al.* [LHCb collaboration], *Measurement of the $B_s^0 - \bar{B}_s^0$ oscillation frequency Δm_s in $B_s^0 \to D_s^-(3)\pi$ decays,* arXiv:1112.4311 [hep-ex].

[4] LHCb collaboration, *First observations and branching fraction measurements of $\bar{B}_s^0$ to double-charm final states,* LHCb-CONF-2012-002.

[5] A. Lenz and U. Nierste, JHEP **0706** (2007) 072.

[6] J. Charles *et al.*, Phys. Rev. D **84** (2011) 033005.

[7] R. Aaij *et al.* [LHCb collaboration], *Determination of the sign of the decay width difference in the B_s system,* arXiv:1202.4717 [hep-ex].

[8] J. Charles *et al.*, Eur.Phys.J. C41, 1 (2005).

[9] M. Ciuchini *et al.*, JHEP 07, 013 (2001).

[10] LHCb collaboration, *Measurement of the $B_s^0 \to J/\psi K_s^0$ branching fraction,* LHCb-CONF-2011-048.

[11] R. Aaij *et al.* [LHCb collaboration], *Measurement of the ratio of branching fractions $\mathcal{B}(B^0 \to K^{\star 0}\gamma)/\mathcal{B}(B_s^0 \to \phi\gamma)$,* arXiv:1202.6267 [hep-ex].

[12] LHCb collaboration, *First observations and branching fraction measurements of $\bar{B}_s^0$ to double-charm final states,* LHCb-CONF-2012-004.

[13] R. Aaij *et al.* [LHCb collaboration], *Observation of CP violation in B^+ to DK^+ decays,* arXiv:1203.3662 [hep-ex].

[14] LHCb collaboration, *Measurement of time-dependent CP violation in charmless two-body B decays,* LHCb-CONF-2012-007.

[15] LHCb collaboration, *Measurement of the CP Violation Parameter A_Γ in Two-Body Charm Decays,* LHCb-CONF-2011-046.

[16] LHCb collaboration, *A search for time-integrated CP violation in $D^0 \to hh^+$ decays,* LHCb-CONF-2011-061.

[17] I. Bigi, A. Paul and S. Recksiegel, JHEP 1106 089 (2011).

[18] A. N. Rozanov and M.I. Vysotsky, *$(\Delta A_{CP})_{LHCb}$ and the fourth generation,* arXiv:1111.6949 [hep-ph].

[19] H. Cheng and C. Chiang, Phys.Rev. D85 034036 (2012).

[20] R. Aaij *et al.* [LHCb collaboration], *Searches for Majorana neutrinos in B^- decay,* arXiv:1201.5600 [hep-ex].

[21] R. Aaij *et al.* [LHCb collaboration], Phys. Rev. Lett. 108 101601 (2012).

[22] LHCb collaboration, *Search for the rare decays $B_s^0 \to \mu^+\mu^-\mu^+\mu^-$ and $B_d^0 \to \mu^+\mu^-\mu^+\mu^-$,*

LHCb-CONF-2012-010.

[23] LHCb collaboration,
Search for the $D^0 \to \mu^+\mu^-$ decay with 0.9 fb^1 at LHCb, LHCb-CONF-2012-005.

[24] R. Aaij *et al.* [LHCb Collaboration],
Physics Letters **B699** (2011) 330.

[25] CDF collaboration, *Search for $B_s^0 \to \mu^+\mu^-$ and $B_d^0 \to \mu^+\mu^-$ Decays in 3.7 fb^{-1} of $p\overline{p}$ Collisions with CDFII*, CDF Public Note 9892.

[26] A. Buras, Acta Phys. Polon. **B41** (2010) 2487.

[27] R. Aaij *et al.* [LHCb Collaboration],
Strong constraints on the rare decays $B_s \to \mu^+\mu^-$ and $B^0 \to \mu^+\mu^-$, submitted to Phys. Rev. Lett., arXiv:1203.4493 [hep-ex].

[28] N. Mahmoudi,
Direct and indirect searches for New Physics, Talk at 47th Rencontres de Moriond on Electroweak Interactions and Unified Theories, 10 - 17 Mar 2012, La Thuile, Italy.

[29] J. Pati and A. Salam,
Phys. Rev. **D10** (1974), 275.

[30] R. Aaij *et al.*, *First observations and branching fraction measurements of $\bar{B}_s^0$ to double-charm final states,* LHCb-CONF-2012-008.

[31] C. Bobeth *et al.*, *More Benefits of Semileptonic Rare B Decays at Low Recoil: CP Violation,* arXiv:1105.0376 [hep-ex].

[32] A. Jaeger *et al., Measurement of the track finding efficiency,* LHCb-PUB-2011-025.

[33] R. Aaij *et al.* [LHCb Collaboration],
Inclusive W and Z production in the forward region at $\sqrt{s} = 7$ TeV, accepted by JHEP, arXiv:1204.1620 [hep-ex].

[34] S. Catani *et al.*,
Phys. Rev. Lett. **103** (2009) 082001.

[35] LHCb collaboration, *Inclusive Drell-Yan production in the forward region at $\sqrt{s} = 7$ TeV,* LHCb-CONF-2012-013.